04,13

Determining the parameters of the LiPON ionic system from the curves of diffusional relaxation of polarization

© A.S. Rudy, M.V. Lebedev, A.V. Novozhilova ¶

Demidov State University,
Yaroslavl, Russia

¶ E-mail: alena.novozhilova.2014@mail.ru

Received March 28, 2023
Revised July 17, 2023
Accepted July 18, 2023

The results of studying the ionic system parameters of the LiPON solid electrolyte by the voltage relaxation method on the polarized Ti|LiPON|Ti structure are presented. The measurements were carried out at temperatures of 223, 248, 273, and 300 K on a bench consisting of a thermostat, a charger, a charge−discharge switching device, and a recording circuit. The samples in the form of Ti|LiPON|Ti test structures charged to a voltage of 1 V were discharged through an external load with a nominal value of 1 MΩ, 100, 10, and 1 kΩ, and 10 Ω curves $U(t)$ were recorded. A mathematical model of diffusion relaxation of polarization is developed, which approximates the discharge curves $U(t)$. The method of fitting the parameters of the approximating dependence was used to determine the equilibrium concentration of lithium ions, the effective thickness of the electrical double layer, and the volume relaxation time of nonequilibrium ions.

Keywords: solid electrolyte, ionic conductivity, polarization, through conduction current, electrical double layer, diffusion.

DOI: 10.61011/PSS.2023.09.57110.47

1. Introduction

Solid-state thin-film lithium-ion batteries (STLIB) form a separate class of chemical current sources. A planar structure and battery production technology based on microelectronics processes serve as a basis for the inclusion in a separate class. The thickness of STLIB functional layers is from 2 to 0.2 μm, therefore, the field strength in the layers is at least two orders of magnitude higher than in conventional batteries. As solid-state electrolyte, most industrial STLIB use lithium phosphorus oxynitride (LiPON) developed by the research team of Oak Ridge National Laboratory [1]. LiPON has advantages over other solid-state electrolytes such as processibility, relatively high conductivity $\sigma = 2 \cdot 10^{-6}\,\mathrm{S \cdot cm^{-1}}$, low electron transference number $t_e < 10^{-8}$, wide operating temperature range and large potential window ~ 5 V. More detailed analysis of LiPON properties, in particular, in terms of strong and weak electrolyte theory is provided in [2].

When manufacturing STLIB, a layer of the solid-state LiPON electrolyte about a micrometer in thickness is applied by vacuum magnetron sputtering of Li_3PO_4 in nitrogen flow. Application procedures are selected such that to ensure amorphous film structure, i.e. the resistance of a nonstoichiometric crystalline film is much higher. According to the LiPON application procedure, the elemental composition of $Li_xPO_yN_z$ film may be varied in rather wide ranges $2.6 \le x \le 3.5$, $1.9 \le y \le 3.8$, $0.1 \le z \le 1.3$ [3]. In traditional thick-film lithium-ion batteries without severe process constraints, crystalline LiPON with stoichiometric composition may be used [2,3]. Crystalline LiPON is produced by synthesis of precursors with molar ratio 1 : 0.2 : 0.3 [4]. The final product as a microcrystalline powder in the form of pressed tables with a density of 78% at 80°C has the conductivity $\sigma = 8.8 \cdot 10^{-7}\,\mathrm{S \cdot cm^{-1}}$, which is sufficiently close to the conductivity of amorphous LiPON [4].

Conductivity is the most important property of the solid-state electrolyte. In the steady charge or discharge state, continuous current flows via the electrolyte, therefore the stationary conductivity of LiPON is of practical interest. In the electrolyte, the ion current is limited by the conductor, therefore charge transfer through the boundaries is possible by means of chemical reactions only. Direct measurements of stationary conductivity will be defined by the reaction rates, rather than by the ion concentration and mobility. Therefore, the conductivity is determined using indirect measurements of alternating current like, for example, in the electrochemical impedance spectroscopy (EIS) method. In [1] and later in [5–7], LiPON conductivity was determined exactly by the EIS method. As an additional method, [1] used the cyclic voltammetry (CVA) method. LiPON voltammogram is basically a current-voltage curve of M|LiPON and LiPON|M contacts (where M is a metal), on which displacement current vs. voltage is overlaid. In this case it is rather difficult to distinguish one current from another and to determine the LiPON conductivity.

Theoretical justification and results of the determination of ion conductor parameters using the conductor polarization relaxation curves (discharge method) are provided herein. This method is close to CVA, but has a significant

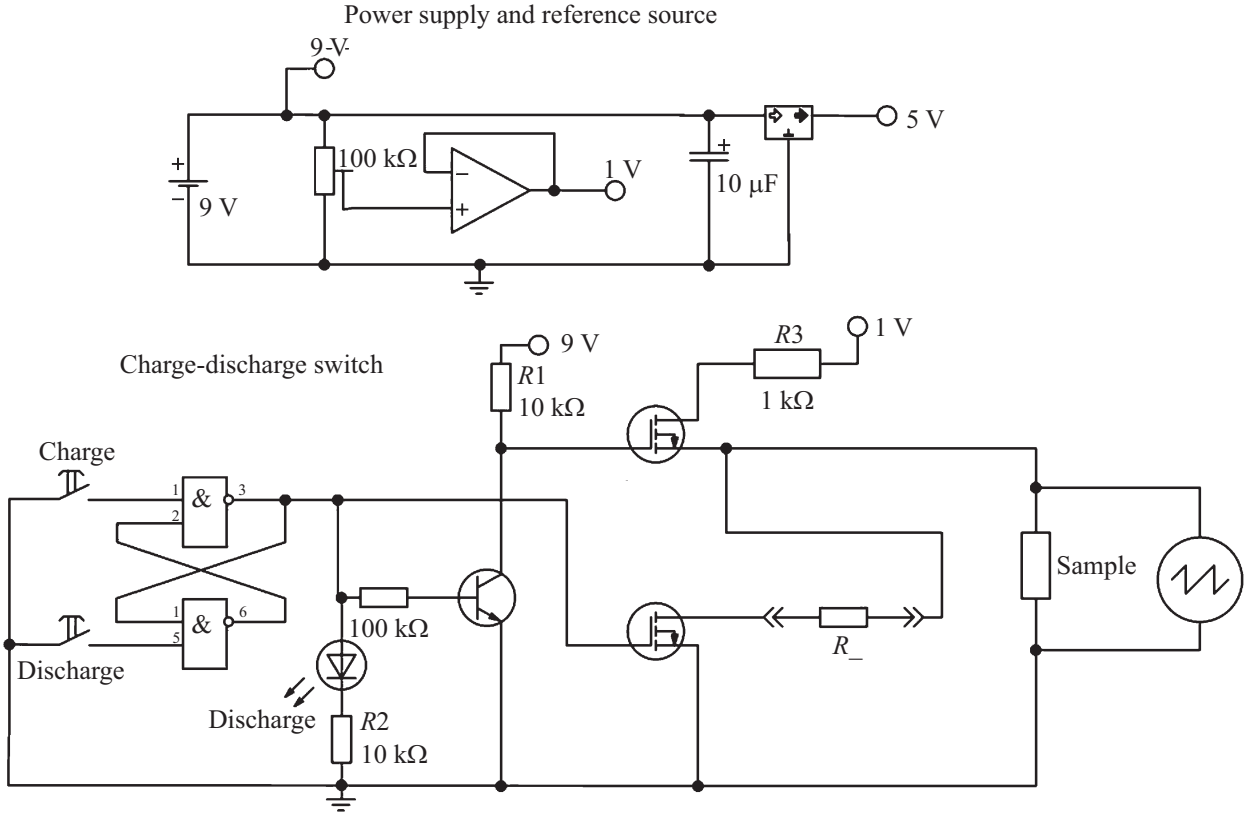

Figure 1. Circuit diagram of a bench for recording charge curves in the test metal−electrolyte−metal structures through an external load.

difference. While according to the EIS and CVA methods the system performs forced oscillations which differ only in the exciting force variation pattern, according to the method of interest the system relaxes towards the equilibrium state under the action of only internal forces. The essence of the method is in recording of voltage on the polarized test $M|\text{LiPON}|M$ structure, where M is the blocking electrode metal. When electrodes M are closed through an external load, diffusional relaxation of the LiPON polarization and simultaneous drain of the charge inductively coupled with LiPON from electrodes (discharge) take place. LiPON ionic system parameters are defined as adjustable parameter of a mathematical model approximating the discharge curves.

An original bench for recording discharge curves of the test Ti|LiPON|Ti structure in the temperature range from −50 to 90°C and measurement procedure are described below. The main discussion is focused on the mathematical modelling (boundary value problem) of diffusional relaxation of LiPON polarization. Solution of the boundary value problem gives an expression approximating the experimental discharge curves $U(t)$. The lithium ion equilibrium concentrations and appropriate LiPON conductivity obtained by fitting are compared with the data from other sources. Based on the temperature dependence of lithium ion concentration and diffusion constant, it was concluded that the solid-state LiPON electrolyte is classified as weal electrolytes.

2. Experiment

Experimental samples with area $1 \times 1\,\text{cm}^2$ and thickness $1\,\mu\text{m}$ were made by magnetron sputtering of lithium orthophosphate in nitrogen atmosphere using SCR-651 Tetra system and constituted a multilayer $\text{Si}|\text{SiO}_2|\text{Ti}|\text{LiPON}|\text{Ti}$ structure, where the layers were listed from bottom to top and where $\text{Si}|\text{SiO}_2$ is the substrate with deposited silicon oxide. The discharge curves were obtained using a bench (Figure 1) consisting of a thermostat, charger, „charge−discharge“ switching system and Hantek 6104 BD digital oscilloscope. The discharge curves were recorded at 223, 248, 273 and 300 K, each measurement consisted of two stages. At the first stage, the sample was held at the pre-defined temperature for 10 min, and then charged with $10\,\mu\text{A}$ up to 1 V. At the second stage, the sample was discharged through an external load. As a load, 1 MΩ, 100, 10 and 1 kΩ, 100 and 10 Ω resistors were used. Charging−discharging modes were switched by transistor switches whose response time was not higher than 50 ns. The discharge curves were recorded using a digital oscilloscope. The sample temperature was maintained using a program-controlled solid-state miniature Peltier element thermostat [8]. Examples of discharge curves for 10 kΩ and 1 MΩ load resistances are shown in Figure 2.

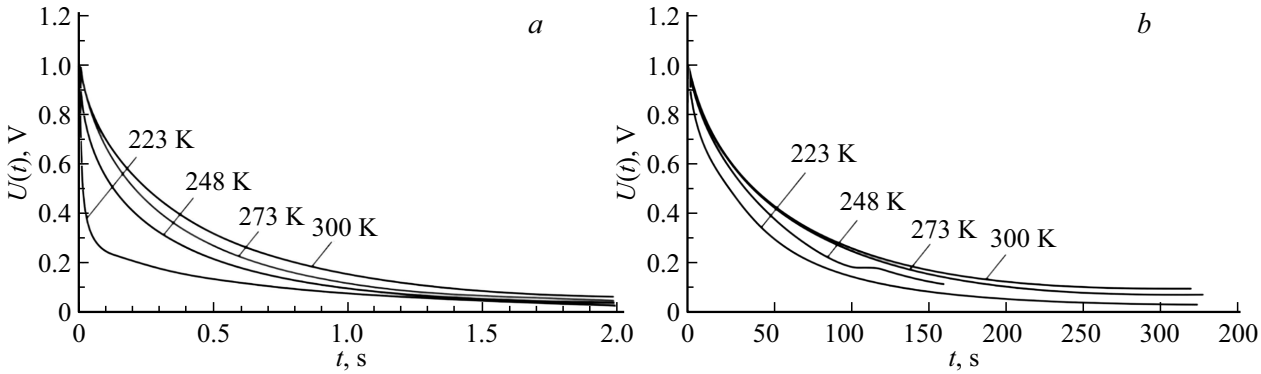

Figure 2. Discharge curves of the test Ti|LiPON|Ti structure through resistances *a*) 10 kΩ and *b*) 1 MΩ at 223, 248, 273 and 300 K.

3. Discharge model

3.1. LiPON polarization in electric field

When DC voltage U_0 is applied to the test sample electrodes, the same process take place in the solid-state electrolyte as in the dielectric. In the external circuit, decaying displacement current is set, which is caused by almost all types of polarization, from which diffusion-interlayer polarization makes the most significant contribution. In the stationary state, the displacement current fades out and only reach-through conductivity current or leakage current is present. The reach-through conductivity current will hereinafter mean the steady-state current or $\lim_{t\to\infty} I(t)$. Transient current will be referred to as the „leakage current". The reach-through conductivity current occurrence mechanism caused by the faradic process and diffusion will be discussed below. It will be only noted herein that this current includes two oppositely directed flows — lithium ions and lithium atoms. Though this is the same element, these particles are not identical, and their isothermal mixing entropy (see, for example, [9]) is not equal to zero. In terms of thermodynamics, the lithium ions and atoms in LiPON form different thermodynamic systems whose chemical potential gradients may be oppositely directed and diffusion constants are different.

3.2. Statement and solution of the initial problem

To determine ion conductivity of the solid-state LiPON electrolyte by the discharge curves, a mathematical model of solid-state electrolyte polarization relaxation is required and shall be constructed using the equivalent scheme. It is sufficiently simple and consists of two capacitors, that simulate the double electrical layer (DEL), connected by Warburg diffused element W and LiPON resistance (Figure 3). All structural elements shown in the diagram, excluding the Warburg element, have lumped parameters and are described by a conventional initial-value differential equation (initial-value problem). The Warburg element has distributed parameters and is described by a boundary-value partial differential equation (boundary value problem). In an earlier model, this element was addressed as a system with lumped parameters [10,11]; therefore, this model contained fewer parameters and was less informative.

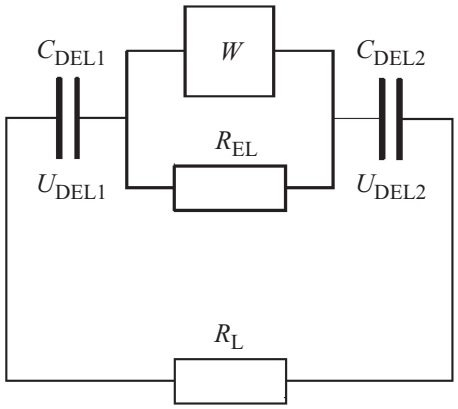

Figure 3. equivalent scheme of the test Ti|LiPON|Ti structure with external load. Here, W is the Warburg diffusion element, R_{El} is the electrolyte resistance, C_{DEL} is the double electrical layer, R_L is the load resistance.

When voltage is applied to the test Ti|LiPON|Ti structure shown in Figure 3, it quickly accumulates the charge on the boundaries due to low thickness of the dense DEL portion. At the same time, slow interlayer-diffusion charge separation takes place within LiPON to compensate the internal residual electric field. Thanks to the absence of electronic charge transfer within the volume, the test structure is able to stay in the polarized state for a long time. When electrodes are closed through an external load, depolarization current is induced in the circuit and the electrode voltage decreases according to $U(t)$, for the curves see Figure 2. To get explicit $U(t)$, the Cauchy problem of electric field relaxation shall be cast and solved.

The electric field strength relaxation equation can be solved by equating the displacement current I_D flowing through the internal circuit section to the current flowing through the external load. The displacement current can be expressed through the electric displacement vector variation

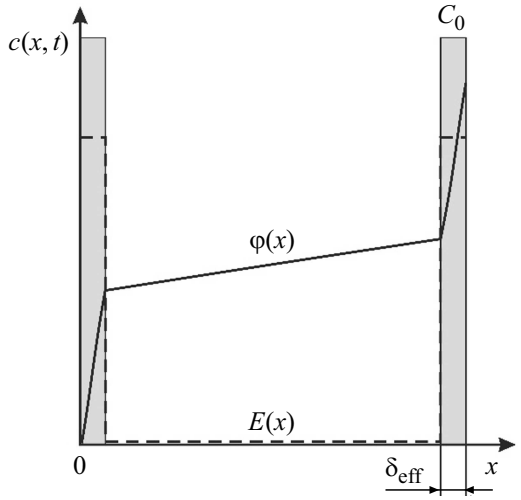

Figure 4. Potential (solid line) and electric field strength (dashed line) distribution in the test structure within the test model.

rate $\mathbf{D} = \varepsilon_0\mathbf{E} + \mathbf{P}$ multiplied by the electrode area

$$I_{\mathrm{D}} \equiv SJ_{\mathrm{D}} = -S\varepsilon_0 \frac{d}{dt} E(t) - S \frac{d}{dt} P(t). \qquad (1)$$

Here, sign „–" before the derivatives is associated with the fact that expression (1) is written in the projection on current direction and the electric strength and polarization moduli derivative is negative in this case. In polarized state of LiPON, the electric field is concentrated mainly inside DEL with thickness δ. The qualitative distribution pattern of the electric field strength $E(x)$ and potential $\varphi(x)$ in DEL within the electrolyte is shown in Figure 4. DEL is further addressed as two endlessly thin charged planes with a gap with thickness δ that remains constant at the specified temperature. In the equivalent scheme (Figure 3), they are represented by C_{DEL1} and C_{DEL2}. It is also assumed that the ion concentration varies during depolarization both in the double electrical layer and within the electrolyte.

Displacement current (1) is equal to the current flowing through the load resistance R_{L}, which may be expressed in terms of voltage on the test structure as $I = U(t)/R_{\mathrm{L}}$. The voltage on the structure is equal to the sum of voltages on the double electrical layer and within the electrolyte:

$$U(t) = U_{\mathrm{DEL1}}(t) + U_{\mathrm{DEL2}}(t) + \int_{\delta}^{d-\delta} E(x,t)dx.$$

According to [11], dielectric constant of LiPON ε_{r} is the quantity of the order of 10^2, i. e. the last term is small (Figure 4) and may be ignored. Since the capacity of the two remaining DELs (air capacitors C_{DEL1} and C_{DEL2}) shall be equal to the test structure capacity, their thickness δ is replaced by the effective thickness δ_{eff}. The effective thickness is selected such that the capacity of the series connection of air capacitors $C_{\mathrm{DEL}}/2 = \varepsilon_0 S/(2\delta_{\mathrm{eff}})$ would be equal to the capacity of the test structure $C = \varepsilon_0\varepsilon_{\mathrm{r}}S/d$. It follows from this condition that

$$\varepsilon_{\mathrm{r}} = d/(2\delta_{\mathrm{eff}}), \text{ a } U(t) = 2E(t)\delta_{\mathrm{eff}}.$$

Then, the external circuit current may be written as

$$I = \frac{E(t)2\delta_{\mathrm{eff}}}{R_{\mathrm{L}}}, \qquad (2)$$

where R_{L} is the load resistance. Equation (1) and relation (2) is reduced to a first-order non-homogeneous linear equation

$$\frac{dE(t)}{dt} + \frac{E(t)}{\tau} = -\frac{1}{\varepsilon_0}\frac{dP(t)}{dt}, \qquad (3)$$

where $\tau = CR_{\mathrm{L}}$ is the time constant RC-chain, and $C = \varepsilon_0 S/(2\delta_{\mathrm{eff}})$ is the capacity of two DELs connected in series (Figure 3). The initial condition for equation (3) is written as

$$E(0) = \frac{U_0}{2\delta_{\mathrm{eff}}}. \qquad (4)$$

Equation (3) is calculated in a standard manner — by the arbitrary-constant variation method. Its solution $E(t)$ is more convenient to write as voltage vs. time

$$U(t) = -\frac{2\delta_{\mathrm{eff}}}{\varepsilon_0} P(t) + \frac{2\delta_{\mathrm{eff}}}{\varepsilon_0\tau} e^{-t/\tau} \int P(t)e^{t/\tau}dt + 2\delta_{\mathrm{eff}}c_0 e^{-t/\tau}, \qquad (5)$$

where c_0 is the integration constant, which is derived from the initial condition (4) and will be explicitly written below. According to (5), the following algorithm step shall be expressing the polarization vector $P(t)$ in terms of non-equilibrium lithium ion concentration $c(x, t)$.

3.3. polarization vector modulus calculation on the assumption symmetrical charge distribution

Further, it is assumed that the charge carrier system in LiPON consists of two types of carriers: holes h^- and lithium ions Li^+. Kinetics of these charge carriers is similar to electron and hole kinetics in intrinsic semiconductors. As in a semiconductor, only positive lithium ions have real mobility in LiPON, and oxygen vacancies O^- are covalently bound with phosphorus atoms. Therefore, holes, whose mobility is mediated by generation and recombination of O^- and Li^+ pairs, rather than cation vacancies, are the second-type carriers. Difference from semiconductors is only in that holes are negatively charged, while activated carriers are positively charged.

To find polarization vs. time, it is natural to assume that lithium ions and holes are initially distributed symmetrically relative to the central plane as shown in Figure 5. Then the charge center defined by the radius vector

$$\mathbf{R}_C = \sum_{i=1}^{2N} \mathbf{r}_i|q_i| \Big/ \sum_{i=1}^{2N} |q_i|,$$

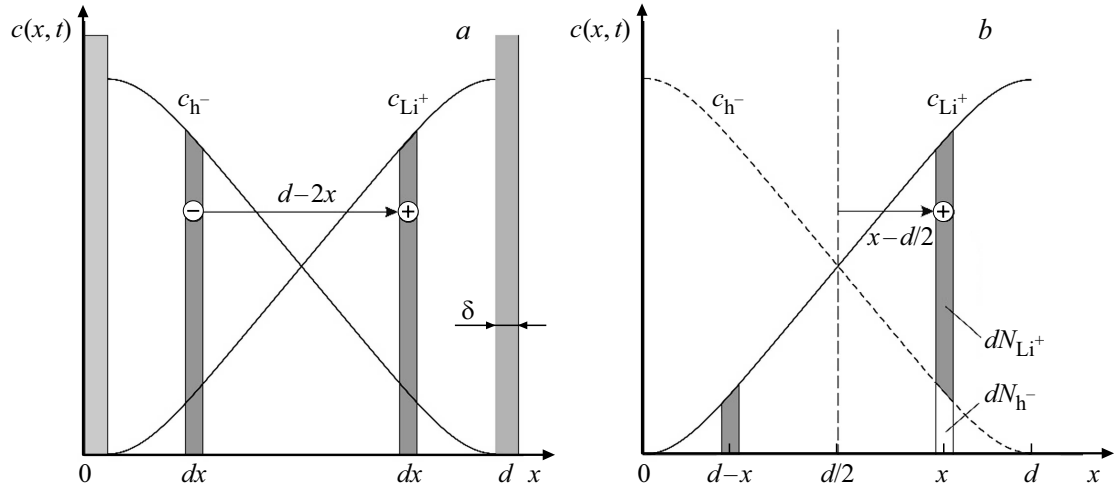

Figure 5. Calculation of polarization with symmetrical distribution of lithium ions and holes: *a*) symmetrical distribution of charges for a arbitrary point of time; *b*) illustration to the dipole moment calculation scheme of layers with thickness dx.

remains in the same point on the central plane during relaxation $c(x,t)$ and $c_{h^-}(x,t)$, because further charge redistribution takes place under internal forces of the closed system. In Figure 5, *a*, the double electrical layer with thickness δ is light-grey. Charge concentration in the elementary layer with thickness dx is dark-grey. Distance between the layers is equal to $d-2x$ — dipole arm, whose moment is equal to $dP = (d-2x)qc(x,t)dx$. To calculate the polarization vector modulus, a more convenient scheme is used, see Figure 5, *b*. According to this scheme, the layer charge dx is calculated as $q[c(x,t)-c_{h^-}(x,t)]dx$, where $c(x,t) = dN_{Li^+}/dx$ is the concentration of non-equilibrium lithium ions in the vicinity of point x, $c_{h^-}(x,t) = dN_{h^-}/dx$ is the concentration of holes in the same point. Owing to the charge distribution symmetry, the hole concentration in point x is equal to the lithium ion concentration in a symmetrical point $c_{h^-}(x,t) = c(d-x,t)$. This allows to calculate the polarization vector modulus for any point of time as

$$P(t) = 2\frac{q}{d}\int_{d/2}^{d}[c(x,t) - c(d-x,t)](x-d/2)dx, \qquad (6)$$

where $x-d/2$ is 1/2 of the dipole moment arm.

Expression (6) allows to find the electrolyte polarization vector for any point of time, if the lithium ion concentration $c(x,t)$ is known. To find the explicit dependence, it is necessary to know the lithium ion distribution within the volume $c(x,t)$. Solution of the appropriate boundary value problem is provided below.

3.4. Space charge diffusional relaxation model

To find the charge distribution function within the electrolyte, boundary value problem of ion diffusion with pre-defined initial distribution shall be solved. Therefore, there is a problem of consideration of free (external) charge field strength. The field of these charges is not included in the test model. It is assumed that after voltage removal free charges (charges on the opposite electrodes inductively coupled with each other and not coupled with electrolyte ions and holes), if any, are quickly drained through the resistor. Thus, throughout the discharge process, the whole field is concentrated within the double electrical layer and within the electrolyte. Apparently, this is not the case for discharge through a load with a higher rating. However, this do not affect considerably the approximation quality, because the type of discharge curve in this case is defined by the last term in (5), for which the relaxation time τ can be easily chosen. In this case, the relaxation time will be a little overestimated and, therefore, the effective thickness of DEL is underestimated. uncertainty of this parameter does not influence the determination accuracy of lithium ion concentration and mobility. With decreasing load resistance, the influence of the last term in (5) decreases and, therefore, the error of determination of the effective double electrical layer thickness is reduced.

When ion generation and recombination processes take place in the electrolyte, then the diffusion equation contains so-called ion „sources“ G and „drains“ R. Ion generation rate G is of activation nature and may be assumed as a constant at the predefined temperature G. The recombination rate depends on the ion concentration and may be written as $R = -C(x,t)/\tau_V$ in the relaxation time approximation, where $C(x,t)$ is the ion concentration, τ_V is the ion concentration relaxation time within the electrolyte. Considering the foregoing, the diffusion equation is written as

$$\frac{\partial C}{\partial t} = D\frac{\partial^2 C}{\partial x^2} - \frac{C}{\tau_V} + G, \qquad (7)$$

where D is the lithium diffusion constant, G is the ion generation rate, and R is the ion trapping rate (for example, lithium ions in cation vacancies) or, in other words, the

charge carrier recombination rate. If the system is open, as in this case, then the ion concentration may be written as a sum of three components: $C(x,t) = C_0 + \bar{c}(t) + c(x,t)$, where C_0 is the equilibrium ion concentration, $\bar{c}(t)$ is the concentration of ions inducing the leakage current or reach-through conductivity at $t \to \infty$, and $c(x,t)$ is the equilibrium ion concentration.

Leakage and reach-through conductivity current ions hereinafter mean those ions which participate in the faradic process on the cathode. Since this process takes place only at the boundary, the ion concentration depends only on time, rather than on the space variable. The leakage current ion concentration may be expressed from the leakage current conductivity for which two relations may be written

$$\bar{\sigma} = \mu q \bar{c}(t), \quad \bar{\sigma} = \frac{I_{lk}(t)}{E(t)S}, \tag{8}$$

where $E(t)$ is the filed strength inside the electrolyte. From (8) and Einstein relation $\mu = Dq/(k_B T)$, it follows that

$$\bar{c}(t) = \frac{I_{lk}(t) k_B T}{Dq^2 E(t) S}. \tag{9}$$

The leakage current, in turn, may be expressed in terms of the faradic process rate in a layer with thickness r_{Li} as

$$I_{lk}(t) = \frac{C(d,t) S r_{Li} q}{\tau_F}, \tag{10}$$

where r_{Li} is the lithium ion radius. Substitution of $E(t) = U(t)/(2\delta_{eff})$ and (10) into (9) give the expression for the leakage current ion concentration

$$\bar{c}(t) = \frac{k_B T r_{Li} 2\delta_{eff}}{DqU(t)\tau_F}. \tag{11}$$

The „reach-through conductivity current“ is relevant for stationary state only, because only then it can be separated from the displacement current. In this case, stationary state corresponds to the initial moment, therefore in (11) time shall be assumed as equal to zero. The equilibrium lithium ion concentration $C_0 = C(d,0)$ may be estimated by expressing conductivity in terms of mobility $\sigma = \mu C_0 q$, and mobility in terms of the Einstein relation $\mu = Dq/(k_B T)$. For common conductivity $\sigma = 2.3 \cdot 10^{-4}\,\mathrm{S/m}$ [1] and diffusion constant $D = 1.5 \cdot 10^{-15}\,\mathrm{m^2/s}$ [12], the equilibrium lithium ion concentration C_0 is $2.5 \cdot 10^{28}\,\mathrm{m^{-3}}$. For the test structure leakage current $5.8 \cdot 10^{-7}\,\mathrm{A}$ determined in [11] and concentration relaxation time $\tau_F = 51.34\,\mathrm{s}$ (with discharge after 1 MΩ, i.e. in quasi stationary state), concentration C_0, according to equation (10), is equal to $2.0 \cdot 10^{28}\,\mathrm{m^{-3}}$. It should be mentioned that this concentration corresponds to the dense portion of the double electrical layer and may exceed the concentration within the volume considerably. Using $C_0 = 2.0 \cdot 10^{28}\,\mathrm{m^{-3}}$ and relation (11), reach-through conductivity current ion concentration may be estimated as $\bar{c}(0) = 9.8 \cdot 10^{29}\delta_{eff}$.

Substitution of $C(x,t) = C_0 + \bar{c}(t) + c(x,t)$ into (7) allows to write the equations for all three ion concentration components

$$G - \frac{C_0}{\tau_V} = 0; \quad \frac{\partial \bar{c}(x,t)}{\partial t} = 0;$$

$$\frac{\partial c(x,t)}{\partial t} = D \frac{\partial^2 c(x,t)}{\partial x^2} - \frac{c(x,t)}{\tau_V}. \tag{12}$$

The first equation gives the expression for the equilibrium ion concentration $C_0 = G\tau_V$. The second equation means that $\bar{c}(t)$ variation rate is equal to zero due to diffusion processes. This is a correct result, because the reach-through conductivity current is by default induced by the electric field. Though the reverse branch of the reach-through conductivity current is diffusional in nature, charge is transferred by atoms that belong to other thermodynamic system.

Thus, only the third equation remains unsolved and shall be added with boundary conditions and initial condition. In this case, these impermeability conditions are a particular case of the Neumann condition. The initial condition assigns such ion distribution $c(x)$, when the sum of diffusion j_{dif} and drift j_{dr} flows at $t = 0$ is equal to zero. The final boundary value problem will be written as:

$$\frac{\partial c(x,t)}{\partial t} = D \frac{\partial^2 c(x,t)}{\partial x^2} - \frac{c(x,t)}{\tau_V}, \tag{13}$$

$$\left.\frac{\partial c(x,t)}{\partial x}\right|_{x=0} = 0, \tag{14}$$

$$\left.\frac{\partial c(x,t)}{\partial x}\right|_{x=d} = 0, \tag{15}$$

$$j_{dr} + j_{dif} = 0. \tag{16}$$

To find the solution of problem (13)–(15), the Fourier method is used, and solution is sought as $c(x,t) = V(x)e^{-\mu^2 t}$, where space variable $V(x)$ — is the eigenfunction of the following operator:

$$\begin{cases} DV''(x) = \dfrac{1-\mu^2\tau_V}{\tau_V} V(x), \\ \left.\dfrac{\partial V(x)}{\partial x}\right|_{x=0} = 0, \\ \left.\dfrac{\partial V(x)}{\partial x}\right|_{x=d} = 0. \end{cases} \tag{17}$$

Solution of the eigenfunction problem for operator (17) is provided in the „Appendix“. Eigenfunction may be represented as a linear combination of basis functions

$$V(x) = a_0 + \sum_{n=1}^{\infty} C_n \cos\left(\pi n \frac{x}{d}\right). \tag{18}$$

Undetermined coefficients C_n of the Fourier series (18) are found from the initial condition of boundary value problem (16), which is stated from the following considerations.

In the initial point of time, i.e. before the transistor switches are switched to load, the system is in the equilibrium state. This means that the local diffusion and drift currents are equal and oppositely directed (16). Accurate calculation of $c(x, 0)$ requires consideration of the local field strength and is associated with cumbersome calculations, therefore a simplified approach is used here. Instead of a local value, an average strength is used

$$\frac{1}{d}\int_0^d [E(x)/\varepsilon_r]dx = U_0/(\varepsilon_r d).$$

Then, drift and diffusion currents may be written as $j_{dr} = \sigma U_0/(\varepsilon_r d)$ and $j_{dif} = -qD[dc(x)/dx]$, and condition (16) may be written as

$$\frac{\sigma U_0}{\varepsilon_r d} - qD\frac{dc(x,0)}{dx} = 0. \quad (19)$$

Here, σ is the ion conductivity of LiPON, and ε_r is the relative dielectric constant taking into account field weakening by the double electrical layers with thickness δ_{eff}. Integration (19) and integration constant determination from condition

$$\int_0^d c(x,t)dx = 0$$

gives the final form of the initial condition

$$c(x,0) = \frac{\sigma U_0}{q\varepsilon_r D}\left[\frac{1}{\pi}\left(\pi\frac{x}{d}\right) - \frac{1}{2}\right]. \quad (20)$$

Function $f(x) = \pi x/d$ in solution (20) can be addressed as a piece continuous function with period $[-d, d]$, which allows to expand the boundary condition into the Fourier series

$$c(x,0) = -\frac{\sigma U_0}{q\varepsilon_r D\pi}\frac{4}{\pi}\sum_{n=0}^{\infty}\frac{1}{(2n+1)^2}\cos\left[\pi(2n+1)\frac{x}{d}\right]. \quad (21)$$

Comparison of (21) with (18) allows to determine the serial coefficients in solution (18):

$$a_0 = 0, \quad C_n = -\frac{4\sigma U_0}{q\varepsilon_r D\pi^2}\frac{1}{(2n+1)^2} \quad (22)$$

and to get the final form of the eigenfunction of operator (17) —

$$V(x) = -\frac{4\sigma U_0}{q\varepsilon_r D\pi^2}\sum_{n=0}^{\infty}\frac{1}{(2n+1)^2}\cos\left[\pi(2n+1)\frac{x}{d}\right]. \quad (23)$$

Since cosine is a bounded function, it follows from (23) that the n-th component of the series tends to zero at $n \to \infty$, i. e. series (23) converges by the D'Alembert criterion.

Components of series (23) damp exponentially with damping decrement μ_n^2, that may be expressed from relation (A.2) provided in the Application

$$\mu_n^2 = \frac{1}{\tau_V} + \frac{\pi^2(2n+1)^2)}{d^2}D. \quad (24)$$

Then the following expression will be the final solution of boundary value problem (13)–(15)

$$c(x,t) = -C_0\frac{4qU_0}{\varepsilon_r k_B T\pi^2}\sum_{n=0}^{\infty}\frac{1}{(2n+1)^2} \times \cos\left[\pi(2n+1)\frac{x}{d}\right]e^{-\mu_n^2 t}, \quad (25)$$

where the conductivity and diffusion constant are replaced by relations $\sigma = \mu C_0 q$ and $D = \mu k_B T/q$. Relaxation of the initial ion distribution to the uniform equilibrium state within model (25) is illustrated on curves in Figure 6.

3.5. Derivation of the approximating discharge curve dependence $U(t)$

Solution (25) allows to calculate the concentration difference

$$c(x,t) - c(d-x,t) = -C_0\frac{8qU_0}{\varepsilon_r k_B T\pi^2}\sum_{n=0}^{\infty}\frac{1}{(2n+1)^2} \times \cos\left[\pi(2n+1)\frac{x}{d}\right]e^{-\mu_n^2 t} \quad (26)$$

in equation (6). Integration (6) gives the explicit dependence of the polarization vector modulus on time

$$P(t) = \frac{16dC_0U_0q^2}{\pi^4\varepsilon_r k_B T}\sum_{n=0}^{\infty}\frac{1}{(2n+1)^4}e^{-\mu_n^2 t}. \quad (27)$$

Substitution (27) into equation (5) allows to determine the integration constant

$$c_0 = E(0) - \frac{16dC_0U_0q^2}{\pi^4\varepsilon_0\varepsilon_r k_B T}\left[\sum_{n=0}^{\infty}\frac{1}{(2n+1)^4}\frac{\tau\mu_n^2}{1-\tau\mu_n^2}\right]. \quad (28)$$

To obtain the final expression form which approximates voltage on the test sample during discharge, it only remains to substitute (27) and (28) into (5):

$$U(t) = U_0 e^{-t/\tau} + \frac{64C_0\delta_{eff}^2U_0q^2}{\pi^4\varepsilon_0 k_B T} \times \sum_{n=0}^{\infty}\left[\frac{1}{(2n+1)^4}\frac{\tau\mu_n^2}{1-\tau\mu_n^2}(e^{-\mu_n^2 t} - e^{-t/\tau})\right], \quad (29)$$

where the relative dielectric constant is expressed in terms of thicknesses $\varepsilon_r = d/(2\delta_{eff})$.

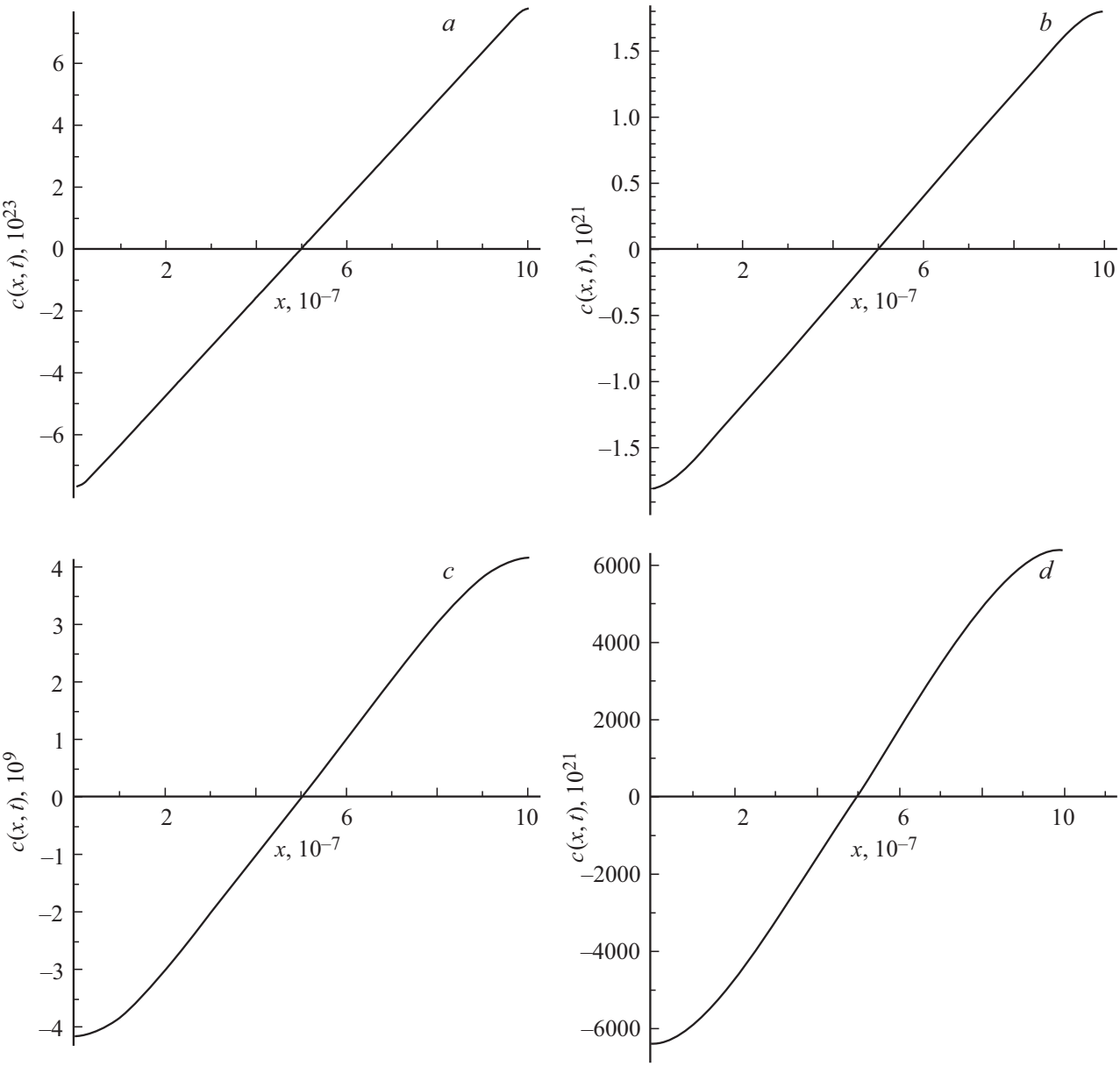

Figure 6. Lithium ion concentration distribution $c(x, t)$ at $C_0 = 2 \cdot 10^{25}\,\mathrm{m}^{-3}$ and $t = a)$ 0.1, $b)$ 1.0, $c)$ 5.0 and $d)$ 7.0 s.

3.6. Approximation of experimental discharge curves

Expression (29) approximates closely the experimental discharge curves (Figure 2). Approximation accuracy is illustrated by curves in Figure 7. The equilibrium lithium ion concentration C_0, effective thickness of the double electrical layer δ_{eff} and non-equilibrium ion concentration relaxation time τ_V were used as adjustable parameters.

4. Discussion of findings

According to the approximation, the equilibrium concentration C_0 is the single parameter which apparently depends on the temperature. The double electrical layer thickness apparently does not depend on the temperature and demonstrates statistical spread relative to the average value $\overline{\delta}_{\text{eff}} = 1.14 \cdot 10^{-10}\,\mathrm{m}$. This value is lower than the covalent radius of the lithium atom $r_{\text{Li}} = 1.34 \cdot 10^{-10}\,\mathrm{m}$, which is allowable for the mathematical model parameter. actually, for the air capacitor to have the same capacity as the test structure with ion conductor, air gap shall be very small. Relative dielectric constant determined as $\varepsilon_{\text{r}} = d/(2\overline{\delta}_{\text{eff}})$ is rather high $\varepsilon_{\text{r}} = 4.39 \cdot 10^3$. The average time of non-equilibrium ion concentration relaxation τ_V does not vary with decreasing temperature and is equal to 0.61 s.

Equilibrium concentration $C_0 = 1.7 \cdot 10^{27}\,\mathrm{m}^{-3}$ at $T = 300\,\mathrm{K}$ is by one order of magnitude lower than $2.0 \cdot 10^{28}\,\mathrm{m}^{-3}$ obtained according to the results in [11]. As mentioned above, this concentration corresponds

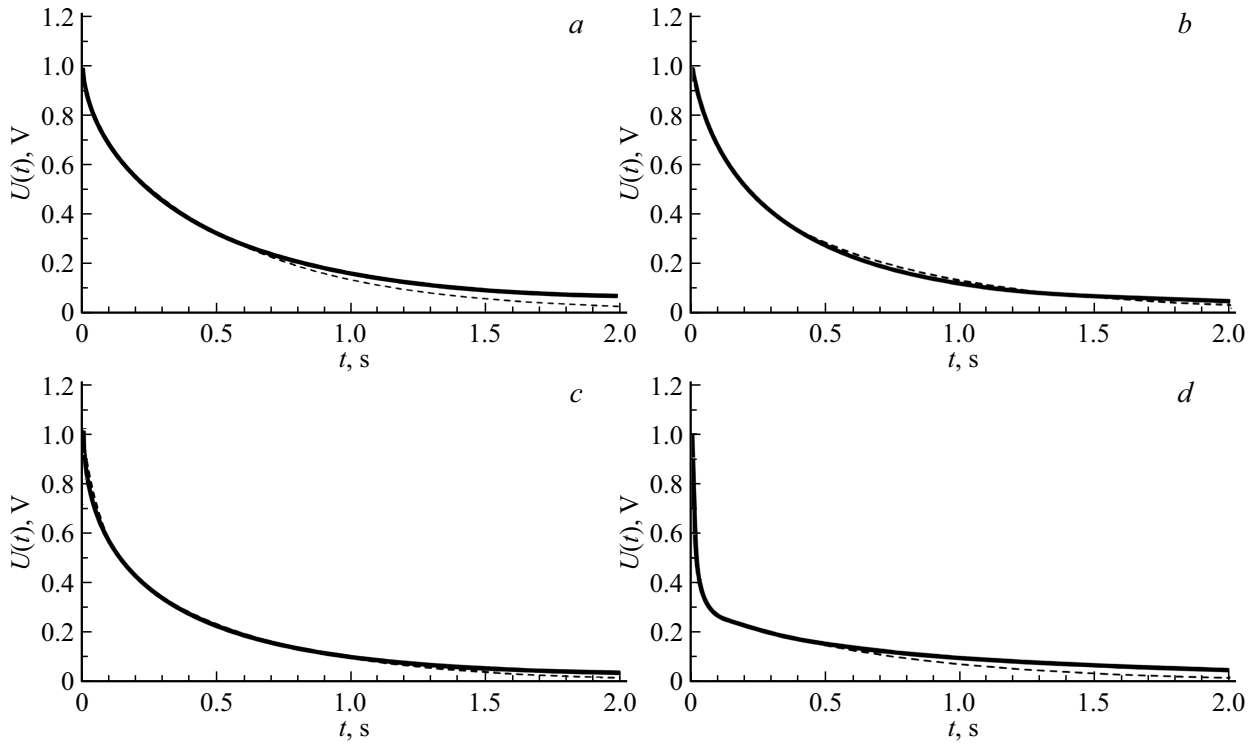

Figure 7. Curves of the test structure discharge through resistance 10 kΩ at different temperatures. Solid line is an experimental curve, dashed line is an approximating curve. Fixed parameters of approximating dependence (33) $U_0 = 1$ V; $D = 1.5 \cdot 10^{-15}\,\mathrm{m}^2 \cdot \mathrm{s}^{-1}$. adjustable parameters: *a*) $T = 300$ K, $C_0 = 1.7 \cdot 10^{27}\,\mathrm{m}^{-3}$, $\delta_{\mathrm{eff}} = 1.2 \cdot 10^{-10}$ m, $\tau_V = 0.55$ s; *b*) $T = 273$ K, $C_0 = 3.5 \cdot 10^{27}\,\mathrm{m}^{-3}$, $\delta_{\mathrm{eff}} = 0.41 \cdot 10^{-10}$ m, $\tau_V = 0.65$ s; *c*) $T = 248$ K, $C_0 = 8.1 \cdot 10^{26}\,\mathrm{m}^{-3}$, $\delta_{\mathrm{eff}} = 0.68 \cdot 10^{-10}$ m, $\tau_V = 0.55$ s; *d*) $T = 223$ K, $C_0 = 6.6 \cdot 10^{25}\,\mathrm{m}^{-3}$, $\delta_{\mathrm{eff}} = 2.3 \cdot 10^{-10}$ m, $\tau_V = 0.70$ s.

to the dense portion of the double electrical layer and may exceed the concentration within the volume. As for deviations from $C_0 = 2.5 \cdot 10^{28}\,\mathrm{m}^{-3}$ derived from the conductivity obtained in [1], the causes of these deviations are of fundamental nature. Actually, in [1], LiPON resistance R was determined as a real component of impedance corresponding to the minimum value of the imaginary component. The fact that $\mathrm{Im}\,\hat{Z} \neq 0$ means that, in addition to the drift current,the diffusion current flows in the electrolyte. Hence, R is not an ohmic resistance, but drift and diffusion current resistance, and $\sigma = \mu C_0 q$ is not applicable in this case. It is easy to see that the ohmic conductivity will be lower than $\sigma = 2.3 \cdot 10^{-4}$ S/m obtained in [1] and the corresponding concentration will be also lower.

On all curves in Figure 7, a minor discrepancy between the asymptotics of the approximating and experimental curves is observed. While the approximating dependence tends to zero, the experimental curves tend to some continuous voltage about 0.3−0.5 V. This may be a sign of the electret effect caused by the space charge with very long relaxation time. relaxation mechanism of this type of polarization is of non-diffusion nature; therefore it is included in the offered model. It is most likely the space charge localized on deep levels, which relaxes slowly due to interlayer-drift charge transfer.

5. Conclusions

Despite some idealization of the ion system within the mathematical model, expression (33) approximates closely the experimental discharge curve. Therefore, it may be assumed that the obtained adjustable parameter values describe the LiPON diffusional relaxation processes adequately. In addition to the parameters mentioned above, expression (33) allows to determine the ion diffusion constant. According to (27), this is possible, if the following condition is satisfied

$$D \geq d^2/\tau_V \pi^2 (2n+1)^2, \tag{34}$$

where $n = 1, 2$. According to [12], for LiPON $D = 1.5 \cdot 10^{-15}\,\mathrm{m}^2/\mathrm{s}$ and condition (34) is satisfied only beginning rom the 5th term of the sum in (33). Therefore, the diffusion constant virtually has no effect on the type of the discharge curve.

Currently, an issue is discussed in the literature regarding the classification of glass-like electrolytes, including also LiPON [2]: strong or weak electrolytes? Conductivity of strong electrolytes is known to be defined by the ion mobility $\sigma = f[\mu(T)]$, $C_0 \neq f(T)$ [13,14], and for weal electrolytes, conductivity depends on ion concentration $\sigma = f[C_0(T)]$, $\mu \neq f(T)$ [15–17]. The approximation mentioned above shows that the ion concentration is a

function of temperature. In this case, the type of discharge curves does not depend on the diffusion constant, but is defined by the bulk relaxation time of non-equilibrium ion concentration due to trapping on cation vacancies. Therefore, the polarization relaxation rate does not depend on the ion mobility as well, because the latter is associated with the diffusion constant by the Einstein relation. Hence, a conservative conclusion may be made that LiPON is a weak electrolyte.

The offered model may be integrated into a more general STLIB model. Charge transfer via the electrolyte during the STLIB discharge is generally similar to the LiPON depolarization. The main difference of the test Ti|LiPON|Ti structure from STLIB is in that the battery electrodes are permeable for lithium due to which their capacities are much higher than those of the double electrical layers. The oxidation-reduction reaction rate at the STLIB electrode boundary is also higher. However, prevalence of diffusion over the drift charge transfer in electrolyte is a feature in common. Therefore, after the appropriate improvement, the offered model may be applicable to the description of STLIB polarization–depolarization which is the main factor determining the battery discharge capacity.

Funding

The study was supported financially by the Ministry of Science and Higher Education of the Russian Federation under state assignment No. FENZ-2020-0006 for Demidov Yaroslavl State University.

Conflict of interest

The authors declare that they have no conflict of interest.

Appendix

Solution of problem (17) is sought in the form $V(x) = e^{\lambda x}$ — of the simplest function satisfying the eigenfunction orthogonality requirement. Its substitution into (17) gives the characteristic equation

$$\lambda^2 = \frac{1 - \mu^2 \tau_V}{D\tau_V}. \qquad (\Pi.1)$$

Roots of this equation may be both real and complex. A single real root $\lambda = 0$ corresponds to the uniform non-equilibrium state $c(t) = c(0)\exp(-t/\tau_V)$, which relaxes to the equilibrium state without space perturbations. Therefore, only the case $1-\mu^2\tau_V < 0$, when roots of the equation (A.1) are complex, is discussed below.

$$\lambda_1 = i\lambda = i\sqrt{\frac{|1 - \mu^2\tau_V|}{\tau_V D}};$$

$$\lambda_2 = -i\lambda = -i\sqrt{\frac{|1 - \mu^2\tau_V|}{\tau_V D}}. \qquad (\Pi.2)$$

Eigenfunction is a linear combination of particular solutions $V(x) = C_1 e^{i\lambda x} + C_2 e^{-i\lambda x}$, from which boundary condition (14):

$$\left.\frac{\partial c(x,t)}{\partial x}\right|_{x=0} = 0 \qquad (\Pi.3)$$

passes only solutions in the form of $V(x) = 2C_1\cos(\lambda x)$. Its substitution into boundary condition (15):

$$\left.\frac{\partial c(x,t)}{\partial x}\right|_{x=d} = 0 \qquad (\Pi.4)$$

gives the equation for operator eigenvalues

$$\lambda \sin(\lambda d) = 0. \qquad (\Pi.5)$$

This equation has an endless number of roots $\lambda_n d = \pm\pi n$, $n = 0, 1, 2, \ldots$, which give a set of eigenfunctions $V_n(x) = C_n\cos(\pi n x/d)$, thus, forming the orthogonal and full basis. Operator eigenfunctions (17) may be expressed in the form of linear combination of basis functions, whereby uniquely

$$V(x) = a_0 + \sum_{n=1}^{\infty} C_n \cos\left(\pi n \frac{x}{d}\right). \qquad (\Pi.6)$$

References

[1] X. Yu, J.B. Bates, G.E. Jellison Jr, F.X. Hart. J. Electrochem. Soc. **144**, *2*, 524 (1997). https://iopscience.iop.org/article/10.1149/1.1837443
[2] Z.A. Grady, C.J. Wilkinson, C.A. Randall, J.C. Mauro. Front. Energy Res. **8**, 218 (2020). https://www.frontiersin.org/articles/10.3389/fenrg.2020.00218/full
[3] P. López-Aranguren, M. Reynaud, P. Gluchowski, A. Bustinza, M. Galceran, J.M. López del Amo, M. Armand, M. Casas-Cabanas. ACS Energy Lett. **6**, *2*, 445 (2021).
[4] K. Senevirathne, C.S. Day, M.D. Gross, A. Lachgar, N.A.W. Holzwarth. Solid State Ionics **233**, 95 (2013). https://doi.org/10.1016/j.ssi.2012.12.013
[5] C.H. Choi, W.I. Cho, B.W. Cho, H.S. Kim, Y.S. Yoon, Y.S. Tak. Electrochem. Solid-State Lett. **5**, *1*, A14 (2020). https://iopscience.iop.org/article/10.1149/1.1420926
[6] F. Tan, X. Liang, F. Wei, J. Du. E3S Web. Conf. **53**, 01008 (2018). https://doi.org/10.1051/e3sconf/20185301008
[7] F. Xu, N.J. Dudney, G.M. Veith, Y. Kim, C. Erdonmez, W. Lai, Y.-M. Chiang. J. Mater. Res. **25**, *8*, 1507 (2010). https://link.springer.com/article/10.1557/JMR.2010.0193
[8] V.A. Zelenkov, M.E. Lebedev, A.S. Rudyi, A.B. Tchurilov. PTE **3**, 142 (2023). (in Russian). https://sciencejournals.ru/view-article/?j=pribory&y=2023&v=0&n=3&a=Pribory2302031Zelenkov
[9] S. Saunders. Entropy **20**, *8*, 552 (2018). https://www.mdpi.com/1099-4300/20/8/552
[10] A.S. Rudyi, S.V. Vasil'ev, M.E. Lebedev, A.V. Metlitskaya, A.A. Mironenko, V.V. Naumov, A.V. Novozhilova, I.S. Fedorov, A.B. Churilov. Tech. Phys. Lett. **43**, *6*, 503 (2017). https://doi.org/10.1134/S106378501706013X.
[11] A.S. Rudyi, M.E. Lebedev, A.A. Mironenko, L.A. Mazaletsky, V.V. Naumov, A.V. Novozhilova, I.S. Fedorov, A.B. Tchurilov. Mikroelektronika, **49**, *5*, 366 (2020). (in Russian). DOI: 10.31857/S0544126920040092

[12] A. Rudy, A. Mironenko, V. Naumov, A. Novozhilova, A. Skundin, I. Fedorov. Batteries **7**, *2*, 21 (2021). https://www.mdpi.com/2313-0105/7/2/21
[13] O.L. Anderson, D.A. Stuart. J. Am. Ceram. Soc. **37**, *12*, 573 (1954). https://ceramics.onlinelibrary.wiley.com/doi/abs/10.1111/j.1151-2916.1954.tb13991.x
[14] H.L. Tuller, D.P. Button, D.R. Uhlmann. J. Non-Cryst. Solids **40**, *1–3*, 93 (1980). https://www.sciencedirect.com/science/article/abs/pii/0022309380900964
[15] D. Ravaine, J.L. Souquet. Phys. Chem. Glasses **18**, *2*, 31 (1977). https://www.researchgate.net/publication/312993493_A_Thermodynamic_Approach_to_Ionic_Conductivity_in_Oxide_Glasses_I
[16] M.D. Ingram, C.T. Moynihan, A.V. Lesikar. J. Non-Cryst. Solids **38**–**39**, *Part 1*, 371 (1980). https://www.sciencedirect.com/science/article/abs/pii/0022309380904470
[17] D. Ravaine. J. Non-Cryst. Solids **38**–**39**, *Part 1*, 353 (1980). https://www.sciencedirect.com/science/article/abs/pii/0022309380904445

Translated by E.Ilyinskaya